# Hartree-Fock directional Compton profiles for diamond

G. G. Wepfer, R. N. Euwema, G. T. Surratt, and D. L. Wilhite*
*Aerospace Research Laboratories, Wright-Patterson Air Force Base, Ohio 45433*
(Received 19 October 1973)

The electron Compton profiles for diamond have been calculated in the impulse approximation from two self-consistent crystalline Hartree-Fock momentum distributions in the [100], [111], [110], [112], and [221] directions. The two calculations use slightly different Gaussian basis sets. The results agree closely with experiment both in magnitude and in directional dependence.

## INTRODUCTION

The emphasis in *ab initio* crystalline calculations is broadening from sole interest in the electron band structure to interest in various ground-state properties as well.[1] Such quantities as the cohesive energy, equilibrium lattice constant, compressibility, x-ray structure factors, and Compton profiles are of interest experimentally and can be computed theoretically with varying accuracy. The cohesive energy depends very sensitively upon electron correlation. This very well-known fact is illustrated in our earlier Hartree-Fock (HF) calculation of diamond[2] in which the HF cohesive energy is 0.38 Ry/atom compared to the experimental value of 0.56 Ry/atom. However, the other energetic quantities (equilibrium lattice constant and compressibility) would be expected to be well represented in the HF approximation from results on molecules. This is borne out by our results on diamond[3] in which the HF lattice constant and compressibility of 3.545 Å and $4.38\times10^{12}$ dyn/cm$^2$ compare closely to the experimental values of 3.567 Å and $4.42\times10^{12}$ dyn/cm$^2$.

The x-ray structure factors and the Compton profiles are derived from the electron first-order density matrix. Since the HF first-order density matrix is stationary to first order, we expect these quantities to be given quite accurately in the HF approximation. The diamond HF x-ray structure factors have been compared with experiment previously. The results were only moderately good (3.26 and 0.08 electrons per crystallographic unit cell compared to the experimental values of 3.32 and 0.14 for the [111] and [222] reciprocal-lattice vectors).

In this paper, self-consistent HF Compton profiles for diamond calculated in the impulse approximation in the [100], [110], [111], [112], and [221] directions, are presented. These results are compared with the experimental results of Weiss and Phillips[4] and of Reed and Eisenberger.[5]

In Sec. II we briefly describe the HF computational model used to generate the results presented in this paper. The working equations for the Compton profile are also presented. In Sec. III, some sample HF results for total energy per atom, virial coefficients, energy bands, and x-ray structure factors are briefly compared to comparable results from our earlier computational model. Then the Compton-profile results are graphed, tabulated, and compared with experiment. Brief conclusions are given in Sec. IV.

## HF COMPUTATIONAL MODEL

The self-consistent crystalline HF computational model used in this paper is a modified version of that described in Refs. 2 and 3. A more complete account of the present model will be described elsewhere. Briefly the method is as follows: local basis functions consisting of four contracted sets of $s$-symmetry Gaussians and three sets of $p$-symmetry Gaussian lobe functions are chosen for each carbon atom. (A Gaussian lobe function of $p$ symmetry consists of two $s$-symmetry Gaussians with equal and opposite coefficients with centers slightly displaced from each other.) These basis functions $\phi_\alpha(r)$ are used to construct Bloch functions:

$$\Phi_\alpha^{\vec{k}}(\vec{r}) = \sum_{\vec{T}} e^{i\vec{k}\cdot\vec{T}}\,\phi_\alpha(\vec{r}-\vec{R}_a-\vec{T}), \tag{1}$$

where the $\vec{T}$ sum is over all crystal translation vectors and $\vec{R}_a$ is a position vector within the unit cell. The same functions are also used to describe the first-order density matrix,

$$\rho_1(\vec{r},\vec{r}') = \sum_{\substack{ab\\ \mu\nu}} A_{\mu\nu}^{ab}\,\phi_\mu(\vec{r}-\vec{R}_a)\,\phi_\nu(\vec{r}-\vec{R}_b), \tag{2}$$

where the $\vec{R}_a$ and $\vec{R}_b$ sums are over all carbon-atom positions in the crystal.

The eigenequations in the Bloch-function basis,

$$F^{\vec{k}}\psi = \lambda U^{\vec{k}}\psi, \tag{3}$$

$$U_{\mu\nu}^{\vec{k}} = \langle \Phi_\mu^{\vec{k}} \,|\, \Phi_\nu^{\vec{k}} \rangle, \tag{4}$$

$$F_{\mu\nu}^{\vec{k}} = \langle \Phi_\mu^{\vec{k}} \Big| -\nabla^2 - \sum_a \frac{2Za}{|\vec{r}-\vec{R}_a|} + \frac{2\rho_1(\vec{r}',\vec{r}')}{|\vec{r}-\vec{r}'|} - \frac{\rho_1(\vec{r},\vec{r}')}{|\vec{r}-\vec{r}'|}\,P_{\vec{r}\vec{r}'} \Big| \Phi_\nu^{\vec{k}} \rangle, \tag{5}$$

where $P_{\vec{r}\vec{r}'}$ interchanges the $\vec{r}$ and $\vec{r}'$ coordinates, are solved separately for each of 19 inequivalent

TABLE I. Contracted Gaussian basis sets. The coefficients $C$ multiply normalized $s$ or $p$ Gaussian lobe functions. Atomic units are used for the exponent $\alpha$ and for $C$.

| | Basis $A$ | | Basis $B$ | |
|---|---|---|---|---|
| | $\alpha$ | $C$ | $\alpha$ | $C$ |
| $1s$ | 16371.1 | 0.000 229 39 | same | |
| | 2439.12 | 0.001 775 27 | | |
| | 545.168 | 0.009 464 79 | | |
| | 151.004 | 0.039 6276 | | |
| | 47.804 | 0.131 291 | | |
| | 16.4357 | 0.320 556 | | |
| $2s$ | 5.949 12 | 0.725 219 | same | |
| | 2.215 88 | 0.310 46 | | |
| $3s$ | 0.85 | 1.0 | 0.75 | 1.0 |
| $4s$ | 0.36 | 1.0 | 0.32 | 1.0 |
| $1p$ | 24.1788 | 0.0408 113 | same | |
| | 5.763 49 | 0.233 71 | | |
| | 1.799 48 | 0.815 897 | | |
| $2p$ | 0.85 | 1.0 | 0.75 | 1.0 |
| $3p$ | 0.36 | 1.0 | 0.32 | 1.0 |

zone points in $\frac{1}{48}$ of the first Brillouin zone. The resulting HF eigenfunctions for the occupied orbitals are then used to construct a new first-order density matrix. This process is iterated to convergence.

Two charge-conserving integral approximations are used in this work for evaluating two-electron integrals. The first approximation, as well as the use of symmetry to reduce the number of one- and two-electron integrals, is described in Ref. 2. The essence of the second integral approximation is that products of diffuse local basis functions are treated at a greater spatial separation than are products of tighter local basis functions. Both of these integral approximations have been tested on molecules in Ref. 6, where they are also fully described. In addition, in this work the monopole and dipole boundary corrections have been replaced by Madelung summation techniques.

TABLE II. Sample computational results for the two basis sets given in Table I. Column $A_1$ gives results from the earlier computational model of Ref. 2. Columns $A_2$ and $B$ give results for the present computational model. All energies are in rydbergs. The $\rho(111)$ and $\rho(222)$ give the (111) and (222) Fourier transforms of the charge density in electrons per crystallographic unit cell. The lattice constant used in all of these calculations is 3.56 Å.

| | $A_1$ | $A_2$ | $B$ |
|---|---|---|---|
| Total energy/atom | −75.7148 | −75.7343 | −75.7393 |
| $-2T/V$ | 1.000 423 | 1.000 513 | 1.000 369 |
| $\rho(111)$ | 3.256 | 3.279 | 3.268 |
| $\rho(222)$ | 0.081 | 0.082 | 0.082 |
| $\Gamma_{25'v}$ | −0.418 | 0.033 | 0.013 |
| $\Gamma_{1v}$ | −2.591 | −2.125 | −2.222 |
| $\Gamma_{15c}$ | 0.636 | 1.109 | 1.053 |
| $X_{4v}$ | −1.037 | −0.572 | −0.621 |
| $X_{1v}$ | −1.767 | −1.302 | −1.314 |
| $X_{1c}$ | 0.820 | 1.149 | 1.028 |

The x-ray structure factors are obtained from the diagonal part of the first-order density matrix

$$S(\vec{k}) = \int \rho_1(\vec{r}, \vec{r})\, e^{i\vec{k}\cdot\vec{r}}\, d\vec{r}, \tag{6}$$

while the electron momentum distribution is obtained from the diagonal part of the full Fourier transform,

$$M(\vec{k}) = \rho_1(\vec{k}, \vec{k}), \tag{7}$$

$$\rho_1(\vec{k}, \vec{q}) = \int e^{i(\vec{k}\cdot\vec{r} - \vec{q}\cdot\vec{r}')} \rho_1(\vec{r}, \vec{r}')\, d\vec{r}\, d\vec{r}'. \tag{8}$$

In the impulse approximation,[7] the Compton profile is then defined as

$$J(q) = \frac{1}{(2\pi)^3} \int \delta\left(\omega - \frac{k^2}{2m} - q\right) \rho_1(\vec{P}, \vec{P})\, d\vec{P}, \tag{9}$$

$$q = \frac{\vec{p}\cdot\vec{k}}{k}.$$

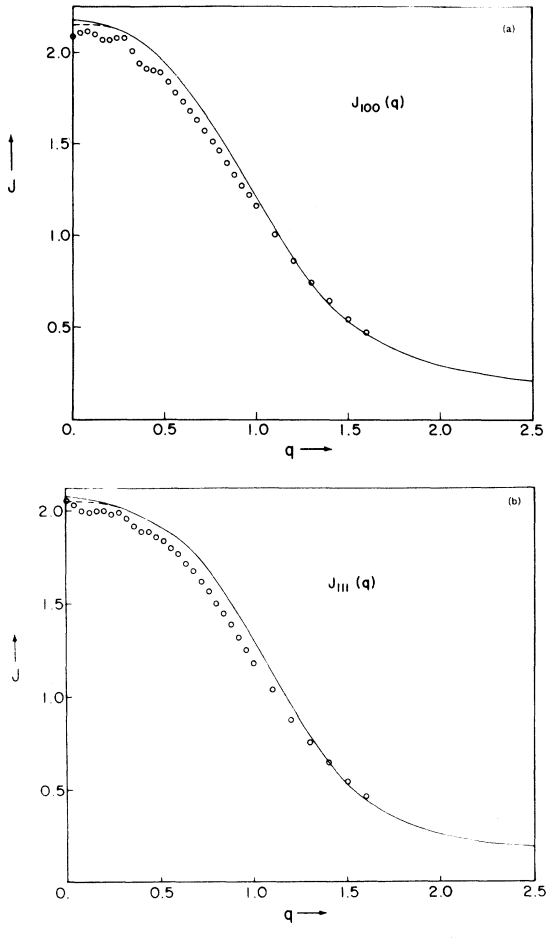


FIG. 1. HF Compton profiles in the impulse approximation are shown for basis set $A$ (the dashed line) and for basis set $B$ (the solid line). The experimental results of Weiss and Phillips (Ref. 4) are shown as circles. They quote an absolute uncertainty of 0.02 $(\text{a.u.})^{-1}$ for all values of $q$.

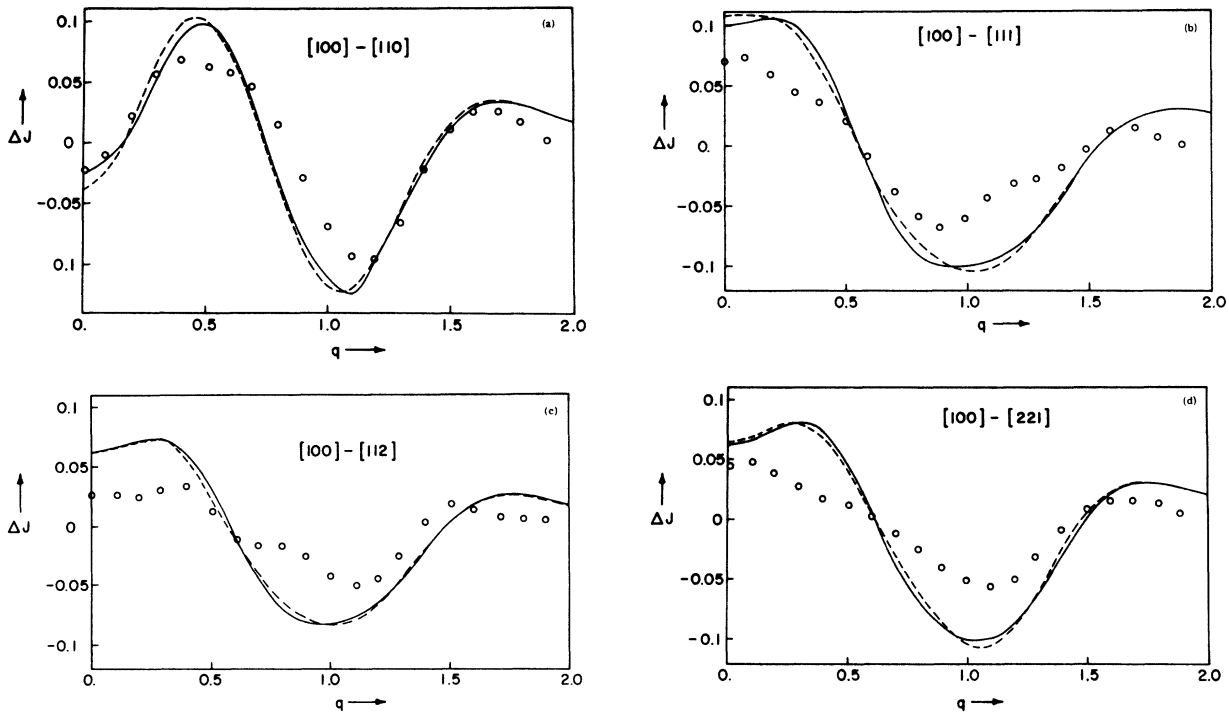


FIG. 2. Differences of HF Compton profiles in the impulse approximation in the designated directions are shown for basis set *A* (dashed line) and for basis set *B* (solid line). The circles give the experimental results of Reed and Eisenberger. These experimental results were taken directly from the graphs in Ref. 5 and are thus not too reliable. Tabulated results were not available for these experiments.

In this equation, $\vec{k}$ gives the change in momentum of the incoming x or $\gamma$ ray, $\vec{P}$ gives the Compton electron momentum. and $\vec{q}$ gives the projection of $\vec{P}$ in the direction of $k$.

TABLE III. Theoretical HF Compton profiles for basis set *B*. Atomic units are used throughout.

| $q$ | $J_{111}$ | $J_{100}$ | $J_{110}$ | $J_{112}$ | $J_{221}$ |
|---|---|---|---|---|---|
| 0.0 | 2.080 | 2.180 | 2.205 | 2.118 | 2.118 |
| 0.1 | 2.070 | 2.173 | 2.187 | 2.108 | 2.106 |
| 0.2 | 2.044 | 2.150 | 2.136 | 2.079 | 2.073 |
| 0.3 | 2.010 | 2.109 | 2.056 | 2.036 | 2.027 |
| 0.4 | 1.972 | 2.046 | 1.959 | 1.985 | 1.972 |
| 0.5 | 1.926 | 1.956 | 1.857 | 1.923 | 1.909 |
| 0.6 | 1.860 | 1.839 | 1.760 | 1.845 | 1.833 |
| 0.7 | 1.765 | 1.700 | 1.670 | 1.745 | 1.736 |
| 0.8 | 1.639 | 1.548 | 1.575 | 1.618 | 1.617 |
| 0.9 | 1.485 | 1.385 | 1.464 | 1.467 | 1.475 |
| 1.0 | 1.316 | 1.216 | 1.325 | 1.298 | 1.316 |
| 1.1 | 1.140 | 1.045 | 1.160 | 1.122 | 1.145 |
| 1.2 | 0.969 | 0.884 | 0.979 | 0.948 | 0.970 |
| 1.3 | 0.807 | 0.742 | 0.802 | 0.787 | 0.802 |
| 1.4 | 0.664 | 0.625 | 0.646 | 0.646 | 0.653 |
| 1.5 | 0.544 | 0.533 | 0.523 | 0.530 | 0.530 |
| 1.6 | 0.449 | 0.460 | 0.432 | 0.441 | 0.437 |
| 1.7 | 0.378 | 0.402 | 0.369 | 0.376 | 0.370 |
| 1.8 | 0.328 | 0.356 | 0.326 | 0.331 | 0.325 |
| 1.9 | 0.292 | 0.320 | 0.297 | 0.299 | 0.293 |
| 2.0 | 0.266 | 0.293 | 0.275 | 0.275 | 0.271 |

The Compton profile in the $z$ direction, i.e., the incoming x or $\gamma$ ray parallel to the crystalline $Z$ axis, is given by

$$J(q) = \frac{1}{(2\pi)^3} \int_{-\infty}^{\infty} dP_x \int_{-\infty}^{\infty} dP_y \times \rho_1(P_x, P_y, q \mid P_x, P_y, q). \quad (10)$$

These integrals can be evaluated analytically in the Gaussian-lobe-function basis.

## RESULTS

We will present theoretical Compton profiles for two separate self-consistent HF calculations with slightly different Gaussian basis sets. By this means we can display the insensitivity of the resulting Compton profiles to the particular choice of basis set. The two basis sets are tabulated in Table I. Basis *A* was used for the lattice-constant and bulk-modulus study of Ref. 3, while basis set *B* employs longer-range outer Gaussians. In order to give the reader an idea of the relation of the present HF results to those of the model in our earlier computations (Refs. 2 and 3), we show some sample computational results in Table II. The total energy per atom has changed only 0.02 Ry/atom from the earlier results, compared to the experimental binding energy of 0.56 Ry/atom. The

virial coefficient (the negative ratio of twice the kinetic energy to the potential energy), has changed little, as have the x-ray structure factors. The HF eigenvalue differences also change little, but the absolute positions of the HF bands have shifted upwards by about 0.45 Ry. We believe this difference to be due to our present use of Ewald summation techniques. We do not believe this is a numerical or computational error since preliminary results on neon using our programs give the same absolute eigenvalues reported by Kunz and Mickish.[8]

The theoretical Compton profiles for the [100] and [111] directions are shown in Fig. 1. The experimental data of Weiss and Phillips are shown as circles on the same graphs. The two theoretical curves are in close agreement for all but the lowest $q$ values. The theoretical curves are slightly higher than experiment at low $q$ values. This same trend is observed for atomic and molecular HF Compton profiles.[9] The curves approach experiment at high $q$ values.

The directional dependences of the Compton profiles are illustrated in Fig. 2 for the five sets of directions measured by Reed and Eisenberger. The two theoretical curves for basis sets $A$ and $B$ again show close agreement. The experimental data is not exactly reproduced by the calculations, but the over-all structure is reproduced. Taking the large (relative to the scale of the graphs of the difference plots) experimental uncertainty into account, the agreement between theory and experiment is excellent.

In order to aid future comparisons with our results, we list the HF Compton profiles for all five directions for basis set $B$ in Table III. We have not subtracted out the contributions of the core states, and we strongly urge others to tabulate results which include core contributions. Experiments measure the entire Compton profile and good calculations also calculate the whole profile, including core contributions.

## CONCLUSIONS

The HF Compton profiles agree very closely with experiment for diamond. The directional dependence measured by Reed and Eisenberger is reproduced. The shapes of the profiles measured by Weiss and Phillips are also reproduced. The magnitudes are slightly higher than experiment for small $q$ values, as reported elsewhere for atomic calculations. We thus conclude that both the computational model and the experimental measurements are confirmed.

While we have thus shown that it is sufficient to use the nonlocal HF exchange operator to obtain good Compton profiles (for diamond at least), it would be interesting to find out whether the nonlocal exchange operator is necessary. We suggest that self-consistent local-exchange-approximation calculations be performed on diamond to see whether they also give good Compton profiles.

---

*National Research Council Postdoctoral Fellow, 1972–1973. Present address: Photo Products Dept., Experimental Station, E. I. duPont deNemours and Co., Wilmington, Del. 19898.

[1]For example, I. Goroff and L. Kleinman, Phys. Rev. B 6, 2574 (1970); F. W. Averill, Phys. Rev. B 4, 3315 (1971); F. W. Averill, Phys. Rev. B 6, 3637 (1971); L. Kumar and H. J. Monkhorst (unpublished); J. Felsteiner, R. Fox, and S. Kahane, Phys. Rev. B 6, 4689 (1972); Refs. 2 and 3.

[2]R. N. Euwema, D. L. Wilhite, and G. T. Surratt, Phys. Rev. B 7, 818 (1973).

[3]G. T. Surratt, R. N. Euwema, and D. L. Wilhite, Phys. Rev. B 8, 4019 (1973).

[4]R. J. Weiss and W. C. Phillips, Phys. Rev. 176, 900 (1968).

[5]W. A. Reed and P. Eisenberger, Phys. Rev. B 6, 4596 (1972).

[6]D. L. Wilhite and R. N. Euwema, Chem. Phys. Lett. 20, 610 (1973).

[7]A discussion of the adequacy of the impulse approximation may be found in P. Eisenberger and P. M. Platzman, Phys. Rev. A 2, 415 (1970).

[8]A. B. Kunz and D. J. Mickish, Phys. Rev. B 8, 779 (1973).

[9]See, for example, P. Eisenberger, Phys. Rev. A 5, 628 (1972); P. Eisenberger and W. A. Reed, Phys. Rev. A 5, 2085 (1972); R. Benesch and V. H. Smith, Jr., Phys. Rev. A 5, 114 (1972).